Synthesis of TPA Impregnated SBA-15 Catalysts and Their Performance in Polyethylene Degradation Reaction

Buğçe Aydemir, Naime Aslı Sezgi, and Timur Doğu
Dept. of Chemical Engineering, Middle East Technical University, Ankara 06531, Turkey

DOI 10.1002/aic.12763
Published online October 21, 2011 in Wiley Online Library (wileyonlinelibrary.com).

Tungstophosphoric acid (TPA)-containing mesoporous santa barbara amorphous (SBA)-15 materials were synthesized by impregnation of TPA into hydrothermally synthesized SBA-15. TPA was incorporated to the porous framework of silica with different W/Si ratios, using TPA hydrate as the acid source. The synthesized materials had a surface area range of 212–825 $m^2 g^{-1}$, depending on the TPA loading and exhibited Type IV adsorption–desorption isotherms. Energy dispersive spectrometry and X-ray photoelectron spectroscopy (XPS) analyses showed that TPA was successfully penetrated into mesopores of the SBA-15 material. Diffuse reflectance infrared Fourier transform spectroscopy (DRIFTS) analysis of the pyridine adsorbed synthesized materials revealed the existence of Lewis and Brønsted acid sites in the synthesized materials. Their performances were tested in the degradation of polyethylene by thermogravimetric analysis. An increase in TPA content significantly lowered the degradation temperature and activation energy of the polyethylene degradation reaction. In the presence of TPA-incorporated SBA-15 catalyst, activation energy was reduced to approximately half-value of the value found in the absence of the catalyst. © 2011 American Institute of Chemical Engineers *AIChE J,* 58: 2466–2472, 2012

Keywords: polyethylene, degradation, tungstophosphoric acid, impregnation, mesoporous material, catalyst, SBA-15

Introduction

Accumulation of nonbiodegradable plastic wastes, which was caused by the mass production of plastic materials, ends up with serious environmental problems. Landfilling method seems to be ineffective, because voluminous plastic materials require a great amount of space and available free space is running out everyday. Incineration of polymers is dangerous and harmful due to the emission of highly toxic chemicals as the product of the reaction. Therefore, extra cleaning treatment units for the effluent gas are required. Polymer cracking seems to be the most promising and sustainable solution to the problem; because by decomposing the polymer, not only the environmental concerns are being eliminated, but also raw materials and fuel-oil-type chemicals are being produced. Degradation of plastic materials can be classified as catalytic and noncatalytic thermal degradation, which are both encouraging in terms of recycling and valuable feedstock recovery.[1]

Although noncatalytic thermal degradation is a possible method, catalytic degradation has many advantages over noncatalytic thermal degradation.[2–4] Decomposition temperature and residence time of the reaction are two important parameters that should be considered, because of energy consumption concerns. By catalytic degradation, it is known that the decomposition temperature and residence time are effectively lowered. The quality and quantity of hydrocarbons produced by degradation are other crucial factors. By catalytic degradation, it is possible to obtain valuable, high-quality light and aromatic hydrocarbons. In thermal degradation, products have wide distribution of molecular weights, requiring further treatment to obtain higher quality hydrocarbons.[5–7]

Catalysts that are commonly used for polymer degradation reactions are solid acid catalysts. These acidic solid catalysts can be classified into several groups such as amorphous aluminosilicates, zeolites, and mesostructured catalysts. Mostly used zeolites are HY,[2,8] ZSM-5,[3,8,9] zeolite Y, and Beta,[10] and so on. Functionality and effectiveness of the catalyst are mostly dependent on the structural properties of the solid. As polymeric molecules are bulky and remarkable in size, the textural properties of the catalysts gain significant importance. The decomposition of the polymer functions over the active site of the catalyst, which is the acid site[11], and access of the polymeric molecule to the active site is mainly controlled by the structure of the catalyst. Zeolites are effective catalysts for degradation reaction in terms of containing acid sites. Main disadvantage of zeolites comes from their microporosity which hinders the access of bulky polymer molecules to the active site of the catalyst. Mesostructured catalysts such as aluminosilicates, mobil composition of matter (MCM)-type and Santa Barbara Amorphous (SBA)-type catalysts on the other hand, have mesopores which allow easier access of the polymeric molecules within the pores of the solid material. However, SBA-15 itself does not show considerable catalytic activity unless appropriate acidic medium is introduced into the structure.[1] Therefore, heteropoly acids can be incorporated to the structure for better catalytic activity. Heteropoly acids are selected as acid source because

Additional Supporting Information may be found in the online version of this article.

Correspondence concerning this article should be addressed to N. Aslı Sezgi at sezgi@metu.edu.tr.

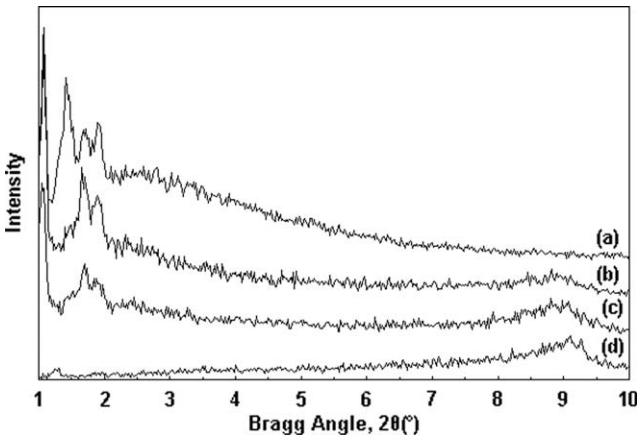

Figure 1. Low angle X-ray diffraction patterns of (a) pure SBA-15, (b) SBA15-0.1, (c) SBA15-0.25, and (d) SBA15-0.40 materials.

of their highly acidic character. Heteropoly acids could not be used alone as catalysts in cracking reactions due to their low thermal stability and surface area.[12] Therefore, they are being used by impregnating into SBA-type silicate catalysts because of high surface area, thermal, and hydrothermal stabilities of these materials.[12] There are very few studies in the literature which use heteropoly acids as the solid acid catalysts in polymer cracking reactions.[13]

In this study, the aim was to develop active, tungstophosphoric acid (TPA)-containing SBA-15 materials with high surface area by impregnation method and to test the performance of these materials in polyethylene degradation reaction by using thermogravimetrical analysis.

Experimental Section

Synthesis of the catalysts

Synthesis of Pure SBA-15 In the synthesis of SBA-15, triblock copolymer (poly(ethylene glycol)-poly(propylene glycol)-poly(ethylene glycol)) (Sigma-Aldrich) and tetraethyl orthosilicate (Merck) were used as the surfactant and the silica source, respectively. SBA-15 catalysts were synthesized following a hydrothermal synthesis route according to the procedure described by Fulvio et al.[14] First, 4 g of surfactant was dissolved in 120 mL of 2M HCl solution and continuously stirred at a rate of 350 rpm at 40°C for 4 h to allow the polymer to be dissolved. Then 8 g of silica source was added dropwise to the solution while stirring and kept stirred for another 2 h. The final solution was transferred into a teflon-lined stainless steel autoclave for the hydrothermal synthesis at 100°C for 48 h. The obtained mixture was filtered and washed with deionized water. The solid product is then dried in the oven and calcined in a tubular furnace at 540°C for 8 h with a flow of dry air to get rid of the organic materials within the pores of the catalyst.

Heteropoly Acid Impregnation to the Presynthesized SBA-15 Materials The recipe given here is a modified version of the procedure described in our earlier study.[15,16] Phosphotungstic acid hydrate (Acros Organics) was used as the TPA source. TPA was introduced to the structure of SBA-15 materials by impregnation method. In this method, first, ~1 g of SBA-15 sample was dispersed in deionized water and kept stirred at room temperature for 2 h. According to the desired W/Si molar ratio, determined amount of TPA was dissolved in deionized water. Then as the SBA-15 solution was being stirred, TPA previously dissolved in water was added dropwise to the solution, and the mixture was kept stirred for 24 h. Finally, water of the mixture was evaporated and the solid product was kept in oven at 110°C for 16 h.

Pure SBA-15 and TPA-impregnated SBA-15 samples were named as PSBA15 and SBA15-X, respectively. X in the notation stands for the W/Si molar ratio of the synthesized material.

Characterization of the catalysts

The synthesized materials were characterized using a variety of techniques. To get information about the regularity of the structure of the synthesized materials was analyzed by X-ray diffraction method. The equipment used for the analysis was Rigaku D/MAX2000 Diffractometer and the Bragg angle values were adjusted in the range of 1°–10° for pure SBA-15 sample and 1°–80° for TPA impregnated SBA-15 samples. The step size was adjusted as 0.01.

The elemental composition of the samples was determined by energy dispersive spectrometry (EDS) analysis using JSM 6400 electron microscope equipped with NORAN system 6 X-ray microanalysis system & Semafore Digitizer.

X-ray photoelectron spectroscopy (XPS) analysis was performed with a monochromatic Al-K_α radiation using a PHI 5000 VersaProbe X-ray photoelectron spectroscopy. Sample was bombarded with 3000 eV Ar^+ ions for 2 min.

Morphology of the catalysts was analyzed using a QUANTA 400F field-emission scanning Electron Microscope and JEOL model JEM 1010 transmission electron microscope equipped with MegaView III CCD camera.

Multipoint Brunauer, Emmett and Teller (BET) surface area, adsorption–desorption isotherms and average pore size of the materials were determined using Quantachrome Autosorb-1C/MS equipment.

DRIFTS spectra of SBA-15 samples were obtained using PerkinElmer-Spectrum One FTIR spectrometer in the wavenumber range of 400–4000 cm^{-1}. Also, to observe the nature of the acid sites of the synthesized materials, DRIFTS analyses of the pyridine-adsorbed samples were performed at room temperature using the same equipment.

Thermogravimetric analysis

To test the performance of synthesized materials in the decomposition reaction of polyethylene, thermogravimetric analysis was carried out using PerkinElmer Pyris 1 thermal gravimetric analysis (TGA). The polymer was polyethylene (Aldrich) of M_n 1700, density 0.92 g mL^{-1}, polydispersity index 2.35, and melting point range 90–110°C.

Thermogravimetric analysis experiments were performed under nitrogen atmosphere having a flow rate of 60 cc min^{-1}, in the temperature range of 30–550°C with a heating rate of 5°C min^{-1}. Testing samples were prepared with a catalyst to polymer weight ratio of 1/2.

Results and Discussion

The X-ray diffraction patterns of pure and TPA containing SBA-15 materials at the low-Bragg angle are shown in Figure 1. The main peak of pure SBA15 sample was at the Bragg angle value of 1.08°. Secondary, tertiary and quaternary peaks were observed at 2θ values of 1.42°, 1.72°, and 1.92° corresponding to the Miller crystal plate (110), (200), and (210), respectively, which match well with the

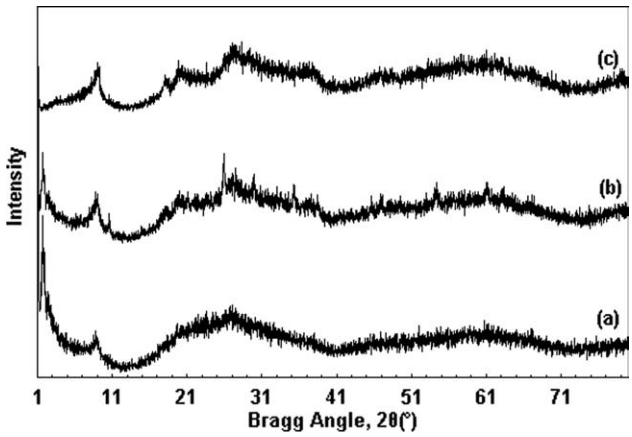

Figure 2. Wide angle X-ray diffraction patterns of (a) SBA15-0.1, (b) SBA15-0.25, and (c) SBA15-0.40 materials.

characteristic pattern of the well-ordered mesoporous structure.[17] For TPA-modified samples, the main peaks were observed at the same Bragg angle value of 1.08°. The intensities of all the peaks decreased with an increasing TPA loading, which results from an increased scattering for filled pores. Disappearance of the second peak and decrease of intensities of all XRD peaks after TPA impregnation are considered to be due to deposition of TPA within the mesopores causing deformations in the ordered structure of the pores. Major distortions in the ordered structure of the material were not observed at low TPA loading. However, for 40% TPA-loaded catalyst, it seemed that its ordered structure was not preserved. On the other hand, transmission electron microscopy (TEM) analysis showed that its ordered structure was not distorted (Figure 6d). In Figure 2, wide angle X-ray diffraction patterns of TPA impregnated materials are given. A broad peak at a Bragg angle value of 24° was observed in all of these materials corresponding to the amorphous structure of silica. TPA-modified materials exhibited a peak at 2θ value of 8.84° which actually is the characteristic peak of TPA and the increase in loading amount caused an increase in intensity of the TPA characteristic peak.

EDS analysis results of TPA impregnated SBA-15 materials are given in Table 1. It was observed that TPA was introduced to the SBA-15 material. This situation was regarded to the wider mesopores of SBA-15 which provide more TPA to pass into the pores of the structure.[1] XPS spectrum of the SBA15-0.1 material is given in Supporting Information Figure S1. XPS result revealed the presence of W on the surface of the sample. The ratio of W to Si was in the same order of magnitude as the W/Si ratio obtained from the EDS results. XPS and EDS results showed that TPA was successfully penetrated into the mesopores of the SBA-15 material.

Nitrogen adsorption–desorption isotherms of synthesized SBA-15 and TPA impregnated SBA-15 materials are shown in Figure 3. According to the International Union of Pure and Applied Chemistry (IUPAC) classification, the synthesized materials exhibited isotherms of Type IV, which is a typical of mesoporous material.[18] H1-type hysteresis was also observed for all of them at a relative pressure range of 0.65–0.80 due to the capillary condensation of nitrogen in the mesopores of the structure, which indicates uniform, narrow pore-size distributions. This hysteresis loop was narrow and the adsorption and desorption branches were quite sharp and nearly parallel in most of the synthesized materials. In Table 2, BET surface area, pore volume, and pore diameter values of the samples are tabulated. Incorporation of TPA to the silica at high loading above 0.25 of W/Si ratio caused a sharp decrease in the surface area values. This sharp decrease might be due to the blocking of synthesized materials' pores by TPA species. Pore diameters which were calculated using Barrett Joyner and Halenda (BJH) model (Table 2) are ~6.5 nm. This indicates the mesoporosity of the material, as expected. All the samples contained considerable amount of micropores, ~24% of the pores. In Figure 4, pore-size distributions of the synthesized materials obtained using BJH model are given. For all samples, pore-size distribution shows a narrow pore diameter range of 2–10 nm, which is again an indication of the mesoporous structure.[18] Hence, TPA loading did not cause a dramatic change in the pore diameter of the samples. On the other hand, pore volume decreased drastically as the amount of TPA loading increased. This situation might be arisen from the fact that TPA molecules were distributed all over the external surface of the silicate structure and blocked the pores.

SEM images of the synthesized samples are given in Figure 5. SEM images of synthesized SBA-15 catalysts revealed the hexagonal array of the material. It was seen that agglomerations were observed in the material when TPA was incorporated to the structure. The loading of TPA did not affect the general shape of the particles. For pure SBA-15 material, the approximate particle size is 0.6 μm, whereas for materials SBA15-0.1 and SBA15-0.40, the measured average particle size values are 0.68 and 0.82 μm, respectively.

TEM images of pure and TPA impregnated SBA-15 materials are shown in Figure 6. As seen from the figure, the

Table 1. EDS Results of Tungstophosphoric Acid-Impregnated SBA-15 Catalysts

Samples	W/Si Ratio (EDS)	W/Si Ratio (in the initial solution)
SBA 15-0.1	0.096	0.1
SBA 15-0.25	0.25	0.25
SBA 15-0.40	0.40	0.40

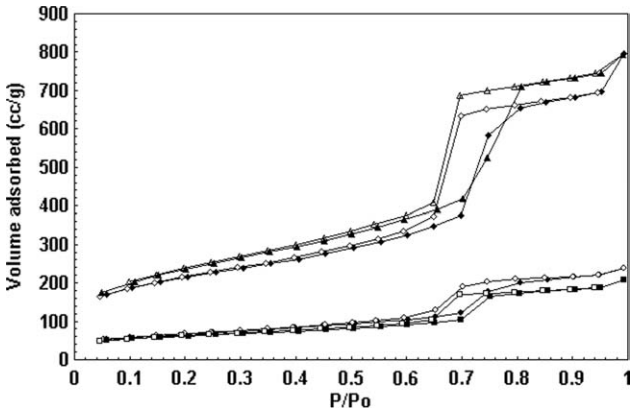

Figure 3. Nitrogen adsorption desorption isotherms of the synthesized materials: rhombus: SBA15-0.1, triangle: pure SBA-15, circle: SBA15-0.25, and square: SBA15-0.40 (filled and empty symbols represent adsorption and desorption branches, respectively).

Table 2. Surface Area and Pore Size Values of the Synthesized Materials

Samples	d_{100}* (nm)	a*,† (nm)	Surface Area "Multi Point" BET (m^2/g)	Pore Volume BJH Des., (cc/g)	BJH Des. Av. Pore Diameter (nm)	Microporosity (%)
PSBA15	8.2	9.4	825	1.18	6.5	23.6
SBA15-0.1	8.2	9.4	749	1.19	6.5	24.4
SBA15-0.25	8.5	9.8	230	0.36	6.6	22.0
SBA15-0.40	–	–	212	0.31	6.5	26.6

*From the XRD results.
†a = lattice parameter.

pores are in honey-comb structure (Figure 6c) and pore channels are arranged very regularly within the particle. The channels are in a cylindrical form (Figures 6a, b, and d) and particles are combined with each other in an ordered manner (Figure 6b). The average measured particle sizes are 0.76 and 0.83 μm for SBA15-0.1 and SBA15-0.40, respectively, and are in a good conformity with SEM images. The distance between two consecutive centers of hexagonal pores was ~10.2 nm. The average wall thickness was ~4.1 nm. The pore diameter was ~6.2 nm.

DRIFTS results of fresh catalysts are given in Figure 7. Peaks obtained at 798 and 886 cm^{-1} are due to W—O_c—W and W—O_b—W stretching vibrations. Here, subscripts b and c stand for the oxygen bridging to W, corner-sharing and edge-sharing belonging to WO_6, respectively.[19] The bands at 968 and 1070 cm^{-1} are assigned to W=O_t and P—O vibrations.[20] These peaks at 798, 886, 968, and 1070 cm^{-1} showed Keggin structure in the synthesized materials.[17] Bands obtained at around 1070 cm^{-1} with a shoulder at 1200 cm^{-1} are due to the asymmetric Si—O—Si stretching vibrations[21] which overlaps with P—O vibration peak and the band at around 798 cm^{-1} is due to Si—O—Si symmetric stretching which overlaps with W—O_c—W[22] stretching vibration peak. Only the TPA peaks at 886 and 968 cm^{-1} are discernable in the spectra of the synthesized materials. In pure SBA-15, the bands at 886 and 968 cm^{-1} were not observed. The intensities of peaks at 886, 968, and 1070 cm^{-1} increased with TPA-loading levels, which indicates incorporation of TPA species to the structure of SBA-15 material and also shows that the Keggin structure is preserved well. A broad peak with a maximum of 3450 cm^{-1} belongs to the hydrogen-bonded silanol groups and adsorbed water.[23] Peak at a wavenumber of 1612 cm^{-1} is assigned to the bending vibration of adsorbed water.[24] The band obtained at 3748 cm^{-1} is due to the existence of free Si—OH (silanol) groups

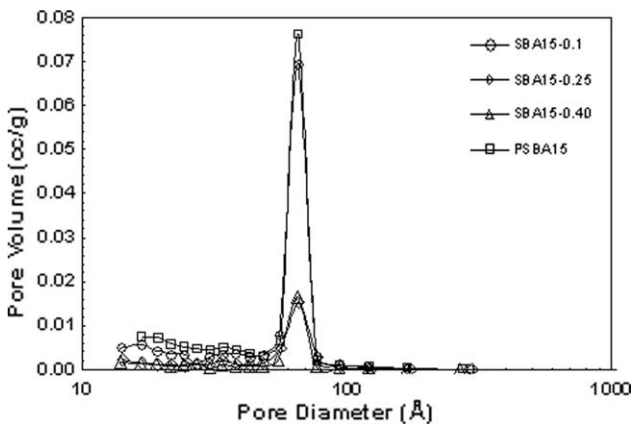

Figure 4. Pore-size distributions of the TPA-loaded SBA-15 materials.

in the material.[23] The band obtained at 3748 cm^{-1} for the pure SBA-15 sample was disappearing as the amount of TPA loaded increased, which may be lost due to the bonding of TPA to those free silanol groups.

To observe the existence of Lewis and Brønsted acid sites in the pure and TPA-modified samples, pyridine was adsorbed on catalysts. The difference between DRIFTS spectra of pyridine adsorbed and fresh catalysts helped to obtain characteristic peaks that give information about Lewis and Brønsted acid sites in the synthesized materials. For instance, bands at 1447 and 1598 cm^{-1} show the existence of Lewis acid sites, whereas bands obtained at 1540 cm^{-1} show the existence of Brønsted acid sites. The band observed at 1489 cm^{-1} is due to the contribution of both Lewis and Brønsted acid sites within the structure.[25] In Figure 8, DRIFTS spectra of pyridine adsorbed samples can be seen. For pure SBA-15 sample, peaks regarding to Brønsted acid sites were not observed, only one band at 1447 cm^{-1} related with the Lewis acid sites in the material was observed.[26] On the other hand, when DRIFTS spectra of all the TPA-impregnated samples are examined, in addition to the aforementioned band obtained due to the Lewis acidity, there are small bands at 1540 cm^{-1} indicating Brønsted acidity. Also, the band at 1489 cm^{-1} is regarded as the contribution of both Lewis and Brønsted acid sites in the structure. Therefore, impregnation of TPA into pure SBA-15 sample led the formation of Brønsted acid sites within the structure and as the amount of TPA increased, the intensities of the peaks regarding to Brønsted acidity were increased.

Figure 9 illustrates the TG analysis under nitrogen flow corresponding to polyethylene in the presence of the synthesized materials. Pure polyethylene shows a steep weight loss in the temperature range of 410–500°C. This steep weight loss arose from the chain degradation. In other words, degradation temperature for pure polyethylene started at 410°C and ended up at 500°C. Those temperatures are very high as the energy consumption for the decomposition reaction is considered. However, in the presence of TPA-impregnated SBA-15, polyethylene shows a steep weight loss at a lower temperature range than in the absence of catalyst. This temperature range shifted to a lower range with an increase in TPA loading. This is the indication of a significant decrease in degradation temperature of polyethylene. It was observed that the acid sites introduced to the structure by impregnation method may play a great role in this decrease. Increase of acidity had a positive effect on the activity of the catalyst for degradation of polyethylene (PE). The increase in the amount of acidity, which is caused by loading of higher amount of TPA, caused a decrease in the polyethylene decomposition reaction temperature. In the presence of catalyst, degradation temperatures of PE corresponding to 10% weight loss are given in Table 3. With an increase in TPA loading, degradation temperature corresponding to 10% weight loss of PE decreases from 323

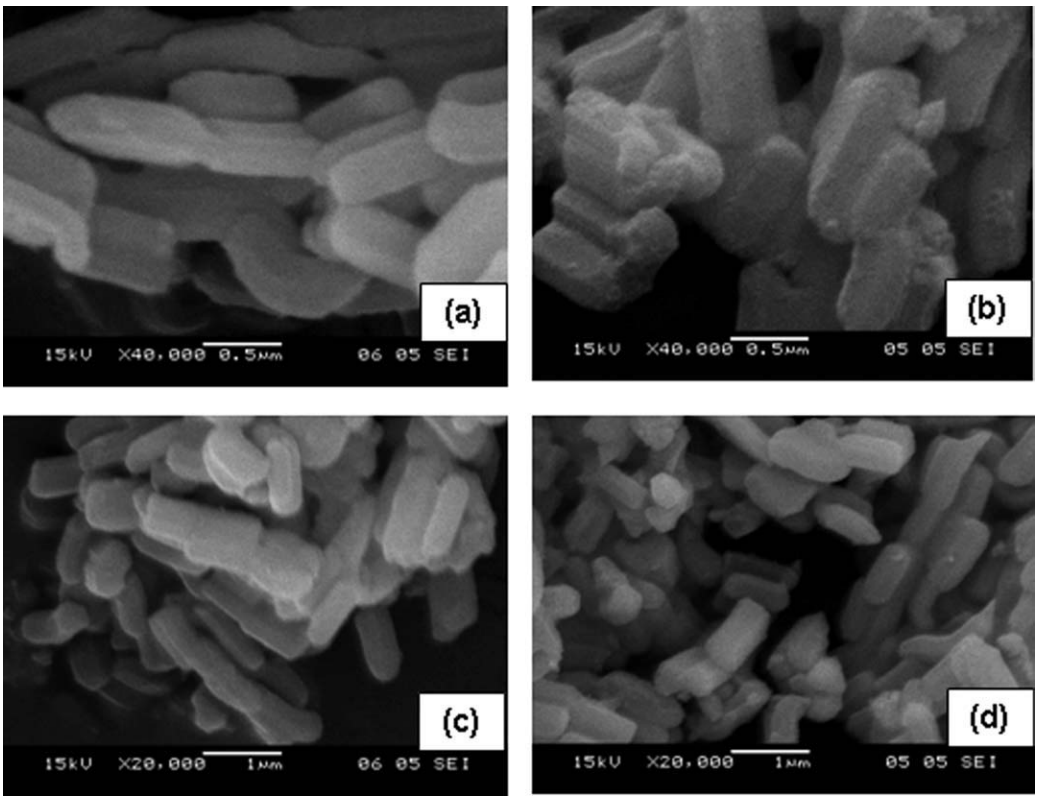

Figure 5. SEM images of (a) SBA15-0.10, (b) SBA15-0.10, (c) SBA15-0.25, and (d) SBA15-0.40.

to 287°C. The weight-loss behavior of polymer in the presence of pure TPA is similar to the weight-loss behavior of polymer in the presence of the SBA15-0.1 material (Figure 9). TGA result in the presence of pure TPA showed that using the SBA-15 support was really beneficial for the polyethylene degradation reaction.

Using the TG data, kinetic parameters for the polyethylene degradation reaction in the presence and absence of these

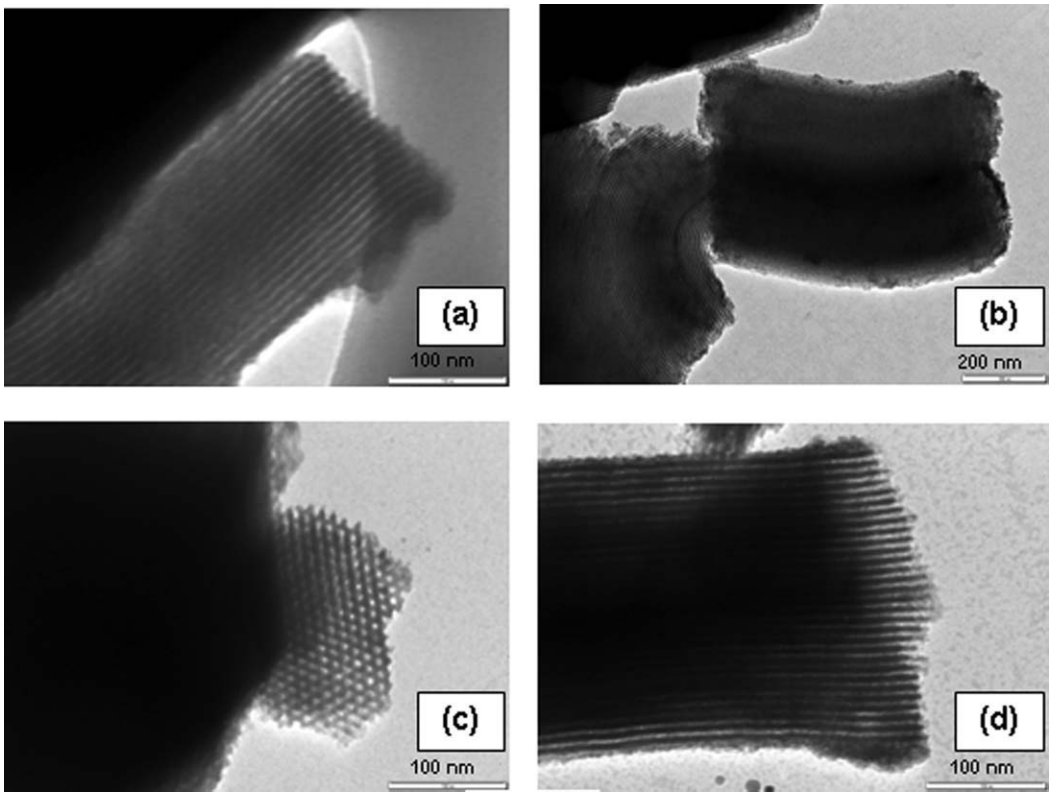

Figure 6. TEM images of (a) pure SBA15, (b) SBA15-0.10, (c) SBA15-0.25, and (d) SBA15-0.40 materials.

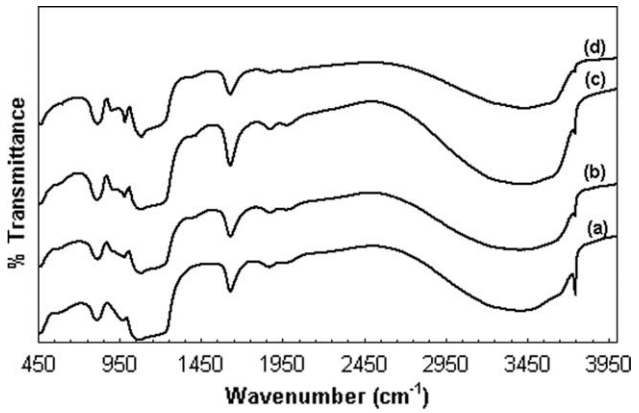

Figure 7. FTIR spectra of the synthesized materials: (a) PSBA15, (b) SBA15-0.1, (c) SBA15-0.25, and (d) SBA15-0.40.

catalysts were evaluated following the procedure reported in our earlier study.[1] A standard power law model was used to describe the kinetics of polyethylene degradation:

$$\frac{d\alpha}{dt} = Ae^{-E/RT}(1-\alpha)^n \tag{1}$$

where A and E are the preexponential factor and activation energy of the reaction, respectively, and n is the overall order of the reaction. α is the fraction of polymer decomposed at time t and defined as follows:

$$\alpha = \frac{w_0 - w_t}{w_o - w_\infty} \tag{2}$$

where w_0, w_t, and w_∞ are the sample weights at time zero, time t, and infinite time, respectively. By inserting a linear heating rate equation ($q = dT/dt$) into Eq. 1 and integrating, it yields,

for the higher order reaction $(n \neq 1)$

$$\ln\frac{1-(1-\alpha)^{(1-n)}}{(1-n)T^2} = \ln\frac{AR}{qE_A} - \frac{E_A}{RT} \tag{3}$$

for first-order reaction$(n = 1)$

$$\ln\frac{-\ln(1-\alpha)}{T^2} = \ln\frac{AR}{qE_A} - \frac{E_A}{RT} \tag{4}$$

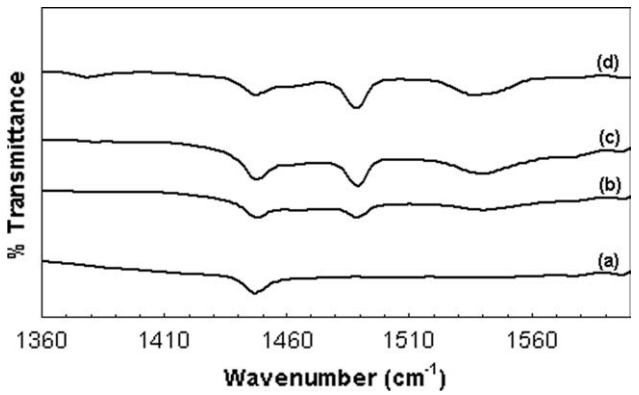

Figure 8. DRIFTS spectra of the pyridine adsorbed catalysts (a) PSBA15, (b) SBA15-0.1, (c) SBA15-0.25, and (d) SBA15-0.40.

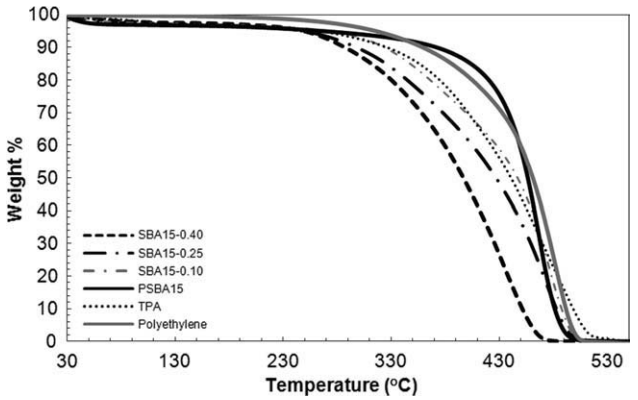

Figure 9. TGA plots of polyethylene in the presence of TPA loaded SBA-15 catalysts.

The overall order of the polyethylene degradation reaction was found to be 1. Activation energy values evaluated from Eq. 4 for PE degradation in the presence and absence of catalysts are tabulated in Table 4. The activation energy for the polyethylene degradation reaction in the absence of the catalyst was ~136 kJ mol^{-1}. The activation energy obtained using TG data is in a good agreement with literature.[27] In the presence of TPA loaded SBA-15 catalyst, when small amount of TPA was incorporated to the SBA-15 material, the activation energy reduced from 136 to 74 kJ mol^{-1}. This might be a proof of importance of Brønsted acid sites in the SBA-15 material for the degradation of PE. With an increase of TPA loading levels, the activation energy further reduced to 62 kJ mol^{-1}. In other words, TPA-modified SBA-15 materials performed a significant activity in decreasing activation energy of the reaction. In the presence of pure TPA, the activation energy value of the reaction was in the same order of magnitude as the activation energy value in the presence of TPA supported on the SBA-15. Gas chromatographic analysis indicated that in the catalytic pyrolysis reaction, the gas product was mainly composed of ethylene. In addition to ethylene, some amounts of propene, ethane, and butane gasses were also observed. In the liquid product, hydrocarbon components were in the range of C8–C14.

Conclusions

In this study, thermally stable, well ordered TPA containing mesoporous SBA-15 materials having different W/Si ratios were successfully synthesized. They exhibited Type IV isotherm with a H1 type hysteresis and had a surface area range of 212–825 m^2 g^{-1}, depending on the TPA loading levels. Their pore diameters were around 6.5 nm which indicated the mesoporosity of these materials. In the XRD patterns of TPA-modified materials, the main peak of pure TPA was also observed. EDS and XPS results showed that TPA was successfully penetrated into the mesopores of the SBA-15 material.

Table 3. Degradation Temperatures of Polyethylene in the Presence of Catalyst at 10% Weight Loss

Catalyst	Temperature (°C)
No catalyst	359
PSBA 15	369
TPA	326
SBA15-0.10	323
SBA15-0.25	298
SBA15-0.40	287

Table 4. Activation Energies for the Polyethylene Degradation Reaction in the Presence of TPA-Impregnated SBA-15 Catalysts

Catalysts	Activation Energy (kJ/mol)
No catalyst	136
PSBA15	161
TPA	66
SBA15-0.10	74
SBA15-0.25	60
SBA15-0.40	62

SEM images revealed the hexagonal structure of the material clearly. TEM images also showed the honeycomb structure of the pores. DRIFTS results revealed the existence of Lewis and Brønsted acid groups and the formation of Brønsted acid sites after the addition of TPA. TPA-modified SBA-15 materials exhibited a significant decrease in the decomposition temperature of polyethylene. The activation energy of the reaction was reduced very effectively, as TPA is a very strong heteropoly acid which then supported by thermally and hydrothermally very stable SBA-15 material to remain without decomposing under high reaction temperatures. Among all the synthesized materials, SBA15-0.25 and SBA15-0.40 showed the best performance in decreasing degradation temperature and activation energy of the PE degradation.

Acknowledgments

The authors thank Middle East Technical University Research Fund (BAP-03-04-2008-08) for the financial support, Central Laboratory of Middle East Technical University for analyses. The authors also thank Dr. Lucian Barbu Tudoran for TEM analysis.

Literature Cited

1. Obalı Z, Sezgi NA, Dogu T. Performance of acidic MCM-Like aluminosilicate catalysts in pyrolysis of polypropylene. *Chem Eng Commun*. 2009;196:116–130.
2. van Grieken R, Serrano DP, Aguado J, Garcia R, Rojo C. Thermal and catalytic cracking of polyethylene under mild conditions. *J Anal Appl Pyrolysis*. 2001;58:127–142.
3. Aguado J, Serrano DP, San Miguel G, Escola JM, Rodriguez JM. Catalytic activity of zeolitic and mesostructured catalysts in the cracking of pure and waste polyolefins. *J Anal Appl Pyrolysis*. 2007;78:153–161.
4. Mikulec J, Vrbova M. Catalytic and thermal cracking of selected polyolefins. *Clean Tech Environ Policy*. 2008;10:121–130.
5. Isoda T, Nakahara T, Kusakabe K, Shigeharu M. Catalytic cracking of polyethylene-liquefied oil over amorphous aluminosilicate catalysts. *Energy Fuels*. 1998;12:1161–1167.
6. Aguado J, Sotelo JL, Serrano DP, Calles JA, Escola JM. Catalytic conversion of polyolefins into liquid fuels over MCM-41: comparison with ZSM-5 and amorphous SiO_2-Al_2O_3. *Energy Fuels*. 1997; 11:1225–1231.
7. Garforth A, Fiddy S, Lin Y-H, Ghanbari-Siakhali A, Sharatt PN, Dwyer J. Catalytic degradation of high density polyethylene: an evaluation of mesoporous and microporous catalysts using thermal analysis. *Thermochim Acta*. 1997;294:65–69.
8. Serrano DP, Aguado J, Escola JM. Catalytic conversion of polystyrene over HMCM-41, HZSM-5 and amorphous SiO_2-Al_2O_3: comparison with thermal cracking. *Appl Catal B-Environ*. 2000;25:181–189.
9. Kaminsky W, Zorriqueta IN. Catalytical and thermal pyrolysis of polyolefins. *J Anal Appl Pyrolysis*. 2007;79:368–374.
10. Chaianansutcharit S, Katsutathi R, Chaisuwan A, Bhaskar T, Nigo A, Muto A, Sakata Y. Catalytic degradation of polyolefins over hexagonal mesoporous silica: effect of aluminum addition. *J Anal Appl Pyrolysis*. 2007;80:360–368.
11. Scheirs J, Kaminsky W. *Feedstock Recycling and Pyrolysis of Waste Plastics: Converting Waste Plastics into Diesel and Other Fuels*. West Sussex: Wiley, 2006.
12. Thomas A, Dablemont C, Basset JM, Lefebvre F. Comparison of $H_3PW_{12}O_{40}$ and $H_4SiW_{12}O_{40}$ heteropolyacids supported on silica by 1H MAS NMR. *CR Chimie*. 2005;8:1969–1974.
13. Jalil PA. Investigations on polyethylene degradation into fuel oil over tungstophosphoric acid supported on MCM-41 mesoporous silica. *J Anal Appl Pyrolysis*. 2002;65:185–195.
14. Fulvio PF, Pikus S, Jaroniec M. Short-time synthesis of SBA-15 using various silica sources. *J Colloid Interface Sci*. 2005;287:717–720.
15. Obalı Z. Synthesis of Aluminum Impregnated Mesoporous Catalysts for Pyrolysis of Polypropylene. Ph.D. Thesis, Middle East Technical University, Ankara, Turkey, 2010.
16. Obalı Z, Sezgi NA, Doğu T. The synthesis and characterization of aluminum loaded SBA-type materials as catalyst for polypropylene degradation reaction. *Chem Eng J*. 2011; doi:10.1016/j.cej.2011.04.063.
17. Kumar GS, Vishnuvarthan M, Palanichamy M, Murugesan V. SBA-15 supported HPW: effective catalytic performance in the alkylation of phenol. *J Mol Catal A-Chem*. 2006;260:49–55.
18. Sing KSW, Everett DH, Haul RAW, Moscou L, Pierrotti RA, Jouquerol J, Siemieniewska T. Reporting physisorption data for gas/solid systems with special reference to the determination of surface area and porosity. *Pure Appl Chem*. 1985;57:603–619.
19. Vazquez P, Pizzio L, Caceres C, Blanco M, Thomas H, Alesso E, Finkielsztein L, Lantano B, Moltrasio G, Aguirre J. Silica-supported heteropolyacids as catalysts in alcohol dehydration reactions. *J Mol Catal A-Chem*. 2000;161:223–232.
20. Sawant DP, Vinu A, Jacob NE, Lefebvre F, Halligudi SB. Formation of nanosized zirconia-supported 12-tungstophosphoric acid in mesoporous silica SBA-15: a stable and versatile solid acid catalyst for benzylation of phenol. *J Catal*. 2005;235:341–352.
21. Holmes SM, Zholobenko VL, Thursfield A, Plaisted RJ, Cundy CS, Dwyer J. In situ FTIR study of the formation of MCM-41. *J Chem Soc*. 1998;94:2025–2032.
22. Zhao XS, Lu GQ, Whittaker AK, Millar GJ, Zhu HY. Comprehensive study of surface chemistry of MCM-41 using ^{29}Si CP/MAS NMR, FTIR pyridine-TPD, and TGA. *J Phys Chem B*. 1997;101: 6525–6531.
23. Brodie-Linder N, Dosseh G, Alba-Simonesco C, Audonnet F, Impéror-Clerc M, SBA-15 synthesis: are there lasting effects of temperature change within the first 10 min of TEOS polymerization? *Mater Chem Phys*. 2008;108:73–81.
24. Liu Q, Wu W, Wang J, Ren X, Wang Y. Characterization of 12-tungstophosphoric acid impregnated on mesoporous silica SBA-15 and its catalytic performance in isopropylation of naphthalene with isopropanol. *Microporous Mesoporous Mater*. 2004;76:51–60.
25. Corma A. Inorganic solid acids and their use in acid-catalyzed hydrocarbon reactions. *Chem Rev*. 1995;95:559–614.
26. Gora-Marek K, Derewinski M, Sarv P, Datka J. IR and NMR studies of mesoporous alumina and related aluminosilicates. *Catal Today*. 2005;101:131–138.
27. Peterson JD, Vyazovkin S, Wight CA. Kinetics of the thermal and therno-oxidative degradation of polystyrene polyethylene and poly (propylene). *Macromol Chem Phys*. 2005;202:775–784.

Manuscript received June 20, 2011, and revision received Aug. 17, 2011.